

## Dispersion interactions between semiconducting wires

Alston J. Misquitta,<sup>1</sup> James Spencer,<sup>2,3</sup> Anthony J. Stone,<sup>2</sup> and Ali Alavi<sup>2</sup>

<sup>1</sup>*Cavendish Laboratory, 19, J J Thomson Avenue, Cambridge CB3 0HE, United Kingdom*

<sup>2</sup>*University Chemical Laboratory, Lensfield Road, Cambridge CB2 1EW, United Kingdom*

<sup>3</sup>*Department of Physics and Thomas Young Centre, Imperial College London, Exhibition Road, London SW7 2AZ, United Kingdom*  
(Received 13 May 2010; revised manuscript received 20 July 2010; published 12 August 2010)

The dispersion energy between extended molecular chains (or equivalently infinite wires) with nonzero band gaps is generally assumed to be expressible as a pair-wise sum of atom-atom terms which decay as  $R^{-6}$ . Using a model system of two parallel wires with a variable band gap, we show that this is not the case. The dispersion interaction scales as  $z^{-5}$  for large interwire separations  $z$ , as expected for an insulator, but as the band gap decreases the interaction is greatly enhanced; while at shorter (but nonoverlapping) separations it approaches a power-law scaling given by  $z^{-2}$ , i.e., the dispersion interaction expected between *metallic* wires. We demonstrate that these effects can be understood from the increasing length scale of the plasmon modes (charge fluctuations), and their increasing contribution to the molecular dipole polarizability and the dispersion interaction, as the band gaps are reduced. This result calls into question methods which invoke locality assumptions in deriving dispersion interactions between extended small-gap systems.

DOI: [10.1103/PhysRevB.82.075312](https://doi.org/10.1103/PhysRevB.82.075312)

PACS number(s): 73.22.-f, 31.15.ap, 34.20.Gj

### I. INTRODUCTION

Conventionally, the dispersion interaction between two systems is formulated in terms of correlated fluctuations described by local (frequency-dependent) polarizabilities which gives rise to the familiar atom-atom  $-C_6^{ab}R_{ab}^{-6}$  interaction at leading order.<sup>1</sup> This form of the interaction has been used with a good measure of success in studies of many systems, from gases to solids, including complexes of biological molecules and organic molecules. These are typically insulators; that is, they have large highest occupied molecular orbital-lowest unoccupied molecular orbital (HOMO-LUMO) gaps.

It has been known for a very long time that the *additive* atom-atom form of the dispersion does not hold very well for metallic systems. The classic case of an atom interacting with a thin metallic surface shows deviations from the additive law: the correct treatment of the metal results in a  $R^{-3}$  power law,<sup>2</sup> but summing over atom-atom terms leads to a  $R^{-4}$  interaction. More recently, strong deviations from additivity have been demonstrated in the interactions of extended systems of metals or zero band-gap materials with at least one nanoscale dimension.<sup>3-7</sup>

The semiclassical picture is useful for understanding the source of the differences in the metallic and insulating cases. In an insulator, electronic perturbations decay exponentially with distance. We can therefore treat electron correlations as being local. At lowest order, these local fluctuations give rise to instantaneous *local* dipoles, and the correlation between these local dipoles gives rise to the atom-atom  $R^{-6}$  interaction. However, in a zero band-gap material, electronic fluctuations are long ranged, particularly if one or two of the dimensions are nanoscale.<sup>3</sup> It is these long-ranged fluctuations that give rise to the nonadditivity of the dispersion and deviations from the atom-atom  $R^{-6}$  interaction.

While the insulating and metallic cases are now well understood, little is known of the intermediate, semiconducting case. The nature of the dispersion interaction between extended molecules with finite but small HOMO-LUMO gaps

less than about 0.2 a.u. (5 eV) remains an open question. A large number of important nanomolecules fall into this category, such as carbon nanotubes and the “lander”-type molecules that are used as organic conductors. The electronic structure of materials made of these molecules depends strongly on structures they assume in the bulk, often via self-assembly. Consequently it is very important to understand exactly how these molecules interact. The dispersion interaction is the dominant source of attraction between these  $\pi$ -conjugated systems. For want of a clearer understanding, many studies assume the usual insulating case for the atom-atom  $R^{-6}$  form of this interaction. As we shall show in this paper, this is both qualitatively and quantitatively incorrect for semiconducting molecules.

A word of clarification: we use the term “nonadditive” here to describe deviations from the additive atom-atom picture of the dispersion interaction between two molecules. It is also commonly used to refer to the deviation from pair additivity seen in the interactions of three or more distinct molecules, but we are not concerned with such effects here, except for a brief comment in the discussion.

### II. INTERACTING WIRES USING HÜCKEL (TIGHT-BINDING) THEORY

The dispersion energy appears at second order in intermolecular perturbation theory and is formally expressed in terms of the exact eigenstates and eigenenergies of the non-interacting systems.<sup>1</sup> In a mean-field theory the dispersion energy between two subsystems (*A* and *B*) can be expressed as a sum over the single-electron wave functions localized to each subsystem

$$E_{\text{disp}}^{(2)} = \sum_{i \in A, j \in B} \sum_{a \in A, b \in B} \frac{|\langle ij | r_{12}^{-1} | ab \rangle|^2}{\epsilon_i + \epsilon_j - \epsilon_a - \epsilon_b}, \quad (1)$$

where  $i, j$  ( $a, b$ ) are occupied (virtual) single-particle wave functions in either subsystem *A* or *B* and  $\epsilon_i$  is the eigenvalue

of the  $i$ th wave function. Assuming two parallel wires, aligned parallel to the  $x$  axis and separated by a distance  $z$ , the integral which appears above has the form

$$\langle ij|r_{12}^{-1}|ab\rangle = \int \frac{\psi_i^*(x_1)\psi_j^*(x_2)\psi_a(x_1)\psi_b(x_2)}{|x_{12}\hat{\mathbf{x}} + z\hat{\mathbf{z}}|} dx_1 dx_2 \quad (2)$$

and is the Coulomb interaction between the charge density  $\psi_i^*\psi_a$  due to excitation  $i \rightarrow a$  in subsystem A with  $\psi_j^*\psi_b$  in B.

In periodic systems, the wave function can be expressed in Bloch form, i.e.,  $\psi_j(x) = e^{ik_j x} u_j(x)$ , and so the codensity  $\psi_i^*(x)\psi_a(x) = e^{i(k_a - k_i)x} u_i^*(x)u_a(x)$  can have a long-wavelength modulation, whose electrostatic field will not be well described by a multipole expansion at separations comparable to this length scale. Furthermore, in small-gap systems, these excitations have plasmon character and contribute significantly to  $E_{\text{disp}}^{(2)}$ , as we discuss below.

Hückel (tight-binding) theory gives us a convenient formalism for evaluating the above expression for interactions between two one-dimensional wires. We considered a two-band model Hamiltonian of the form

$$H = \sum_i^n (\beta a_{2i}^\dagger a_{2i-1} + \beta' a_{2i+1}^\dagger a_{2i} + \text{H.c.}), \quad (3)$$

where  $\beta, \beta'$  are alternating bond strengths between adjacent sites, as would be encountered in a chain of  $(\text{H}_2)_n$  or a  $\pi$ -conjugated polyene. We computed the interactions between two such parallel wires, each consisting of  $2n$  identical atoms, equally spaced at intervals of  $d$ , such that the unit cell is of length  $2d$  and contains two atoms. Assuming periodic boundary conditions over a crystal cell of length  $2dn$ , then there are two bands per wave vector. The single-particle wave functions and energies of such a system can be found analytically. The band structure is given by

$$\epsilon(k) = \pm |\beta e^{ikd} + \beta' e^{-ikd}| \quad (4)$$

and the set of wave vectors by

$$k = \frac{\pi j}{nd}; \quad j = -\frac{n}{2} + 1, -\frac{n}{2} + 2, \dots, \frac{n}{2}. \quad (5)$$

$\beta = \beta'$  corresponds to a uniform wire with energy eigenvalues given by  $\epsilon(k) = \pm 2\beta |\cos(kd)|$ , which in the limit of large  $n$  has a vanishing band gap at half filling (i.e., is a metal). The opposite limit ( $\beta' = 0$ ) corresponds to a chain of isolated dimers with energy eigenvalues  $\epsilon(k) = \pm \beta$ , independent of wave vector, and corresponds to the perfect insulator. By varying the ratio  $\beta'/\beta$  between 0 and 1, we can very conveniently probe the dispersion interaction in the intermediate (semiconducting) regime with the band gap given by  $\Delta E_g = 2(\beta - \beta')$ . The required integrals can be evaluated<sup>8</sup> as

$$\langle ij|r_{12}^{-1}|ab\rangle = \frac{1}{nd} \sum_G K_0(Gz) Y_{ia}(G) Y_{jb}(k_i + k_j - k_a - k_b - G), \quad (6)$$

where  $\{G\}$  are reciprocal lattice vectors of the primitive unit cell and  $Y_{ia}(G)$  is the (analytic) Fourier transform of  $u_i^* u_a$  obtained by assuming highly localized basis functions on

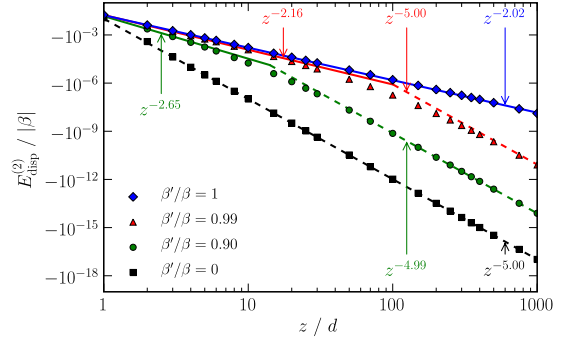


FIG. 1. (Color online) The second-order dispersion energy of parallel wires modeled using Hückel theory obtained from Eq. (1). The bonding interaction is of alternating strength and is controlled by the ratio  $\beta'/\beta$ . The lines are numerical power-law fits to the small- $z$  and large- $z$  data points. In the metallic ( $\beta = \beta'$ ) and perfect insulating ( $\beta' = 0$ ) cases, a single power-law fits the whole range of  $z$  with the expected exponents  $-2$  and  $-5$ , respectively. The intermediate cases show a crossover between these two limiting regimes as  $z$  is varied.

each atom.  $K_0$  is the zeroth-order-modified Bessel function of the second kind and is the Fourier transform of the potential generated by a one-dimensional lattice at a field point at  $z$  from the lattice.<sup>9-11</sup>  $K_0$  decays exponentially with increasingly large arguments and so typically only the ten smallest reciprocal lattice vectors need to be included in the summation in order to obtain converged results.

The calculations presented here use 8401 Monkhorst-Pack  $k$  points to sample the Brillouin zone, which corresponds in real space to wires consisting of 16 802 sites per crystal cell. Such fine  $k$ -point sampling was required to obtain converged results with respect to system size.

As shown in Fig. 1, the dispersion interaction between two uniform wires ( $\beta'/\beta = 1$ ) varies as  $\sim z^{-2}$  across the whole range of  $z$ , in good agreement with previously obtained results via random-phase approximation<sup>3</sup> and quantum Monte Carlo<sup>7</sup> calculations for metallic wires. The interaction between chains of isolated dimers ( $\beta' = 0$ ) varies as  $z^{-5}$ , as would be expected from the conventional picture of dispersion interactions. In the semiconducting regime, there is no unique exponent which characterizes the dispersion interaction over all  $z$ . However, at small separations  $z$ , it tends to the metallic behavior ( $z^{-2}$ ) whereas large  $z$  it tends to insulating behavior  $z^{-5}$ .

### III. INTERACTING H<sub>2</sub> CHAINS USING SAPT(DFT)

The principal drawback of the Hückel model is the lack of electron correlation, and hence screening, within each subsystem. For more realistic calculations we can use the symmetry-adapted perturbation theory based on density-functional theory<sup>12-14</sup> [SAPT(DFT)], where the dispersion energy is evaluated not via a sum over states but through a coupled Kohn-Sham formulation based on the density-response functions of the interacting molecules<sup>15</sup>

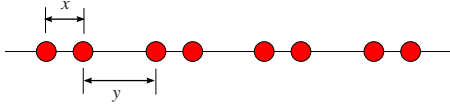


FIG. 2. (Color online) Distorted  $(\text{H}_2)_n$  chains. The distortion parameter is defined as  $\eta=y/x$ . In all our chains we have chosen  $x=1.4487$  a.u.

$$E_{\text{disp}}^{(2)} = -\frac{1}{2\pi} \int_0^\infty dw \int d\mathbf{r}_1 d\mathbf{r}'_1 d\mathbf{r}_2 d\mathbf{r}'_2 \times \frac{\alpha_A(\mathbf{r}_1, \mathbf{r}'_1; iw) \alpha_B(\mathbf{r}_2, \mathbf{r}'_2; iw)}{|\mathbf{r}_1 - \mathbf{r}_2| |\mathbf{r}'_1 - \mathbf{r}'_2|}, \quad (7)$$

where  $\alpha_{A/B}(\mathbf{r}, \mathbf{r}'; w)$  are the frequency-dependent density-response functions of the molecules which describe the propagation of a frequency-dependent perturbation in a molecule, from one point to another, within linear-response theory. The second-order dispersion energy is exact in this formulation if exchange effects are neglected.

We have studied the interactions between two parallel finite  $(\text{H}_2)_n$  (Fig. 2) chains with  $n=16$  and 32 and distortion parameters  $\eta=2.0, 1.5, 1.25$ , and 1.0, where  $\eta$  is the ratio of the alternate bond lengths. The HOMO-LUMO gap of a hydrogen chain can be modified by simply introducing a difference in alternate bond lengths. The distortion parameter  $\eta$  gives us a convenient way to control the electronic structure of the chain and allows us to study the interactions between insulating, semiconducting, and (near) metallic chains in one framework.

The frequency-dependent density-response functions that appear in Eq. (7) were evaluated with coupled Kohn-Sham perturbation theory, using the PBE0 functional<sup>16</sup> with a hybrid kernel consisting of 75% adiabatic local-density approximation and 25% coupled Hartree-Fock (HF). The accuracy of this approach for the dispersion energy of small molecules surpasses that of Møller-Plesset perturbation theory and rivals that of coupled-cluster methods.<sup>13–15,17,18</sup> Furthermore, there is no qualitative change in our results when the fraction of HF exchange is increased, so the results presented here are unlikely to be artifacts of the shortcomings of coupled Kohn-Sham perturbation theory.<sup>19,20</sup> All calculations used the cc-pVDZ basis<sup>21</sup> which will result in a significant underestimation of the strength of the contribution to the dispersion energy that arises from transverse polarization, but should better describe the contribution arising from the longitudinal polarization. Since it is the longitudinal polarization that is most important in these systems, we expect our results to be qualitatively correct.

Dispersion energies are displayed in Fig. 3 and the effective power laws for the physically important separations between 6 and 20 a.u. are shown in Table I together with HOMO-LUMO gaps. For insulating chains with an additive dispersion interaction we would expect two regimes determined by chain length  $L$ : for  $z \ll L$  we should expect the infinite chain result, i.e., the effective dispersion interaction should decay as  $z^{-5}$ , and for  $z \gg L$  we should recover the usual  $z^{-6}$  power law. This is what we see with the chains with

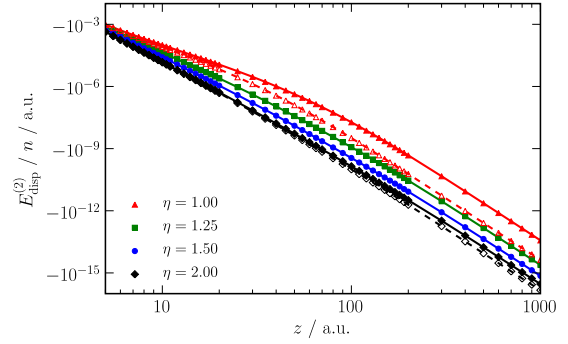


FIG. 3. (Color online) The second-order dispersion energy of pairs of parallel  $(\text{H}_2)_n$  chains. Energies have been normalized by the number of  $\text{H}_2$  units  $n$ . The solid lines are dispersion energies for chains with  $n=32$  and the dashed lines for chains with  $n=16$  (only  $\eta=1.0$  and 2.0).

the largest distortion parameter,  $\eta=2.0$ , which exhibit large HOMO-LUMO gaps. As the distortion parameter  $\eta$  approaches unity and the HOMO-LUMO gap consequently decreases, the deviation from the additive insulating case becomes increasingly apparent, and for the longest of the chains considered here the dispersion interaction is significantly enhanced. For example at 40 a.u. (roughly half the chain length) an  $\eta=1$  chain has a dispersion interaction two orders of magnitude larger than an  $\eta=2$  chain. Additionally, we see increasing finite-size effects: the power laws for the  $n=16$  and 32 chains, which were very similar for  $\eta=2.0$ , are considerably different for  $\eta=1.0$ .

#### IV. MULTIPOLE EXPANSION

We can understand these effects in terms of the multipole expansion. The multipole form of the dispersion energy is usually formulated in terms of (local) atomic polarizabilities. This leads to the usual  $R^{-6}$  atom-atom interaction (at leading order) and would not account for the anomalous dispersion power laws that we have observed in the chains. However the complete distributed-polarizability description is nonlocal: that is, it describes the change in multipole moments at one atom in response to a change in electrostatic fields at another.

TABLE I. Power-law behavior of  $E_{\text{disp}}^{(2)}$  fitted to the form  $z^{-x}$  in the region from 6 to 20 a.u. Beyond 600 a.u. all chains exhibit dispersion energies with the  $z^{-6}$  power law because of their finite length. The HOMO-LUMO gaps,  $\Delta E_g$ , have been calculated from the Kohn-Sham eigenvalues. Energies are in atomic units.

$\eta$	$(\text{H}_2)_{16}$		$(\text{H}_2)_{32}$	
	$\Delta E_g$	$x$	$\Delta E_g$	$x$
2.0	0.370	4.89	0.366	4.84
1.5	0.280	4.58	0.270	4.50
1.25	0.202	4.20	0.183	4.09
1.0	0.099	3.52	0.057	3.17

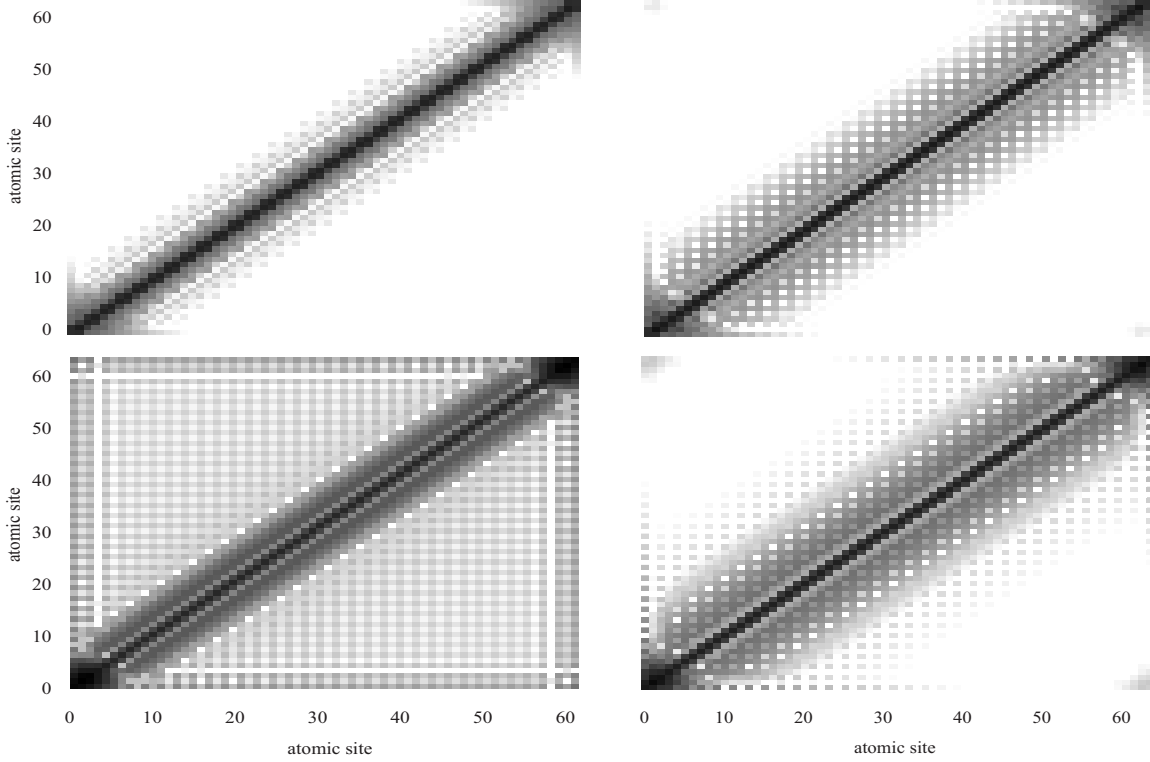


FIG. 4. Matrix representation of the charge-flow polarizability matrix  $\alpha_{00,00}^{aa'}$  for  $(\text{H}_2)_{32}$  chains with  $\eta=2, 1.5, 1.25$ , and 1 (clockwise, from top left). Sites  $a$  and  $a'$  are represented along the  $x$  and  $y$  axes. Because these terms span a number of orders of magnitude of both signs we have plotted  $\ln(|\alpha_{00,00}^{aa'}|)$ . Color scheme: Black rectangles correspond to terms of order 1 a.u. and white rectangles to terms of order  $10^{-3}$  a.u.

We obtain the multipole form of Eq. (7) by expanding the Coulomb terms using the distributed form of the multipole expansion  $|\mathbf{r}-\mathbf{r}'|^{-1}=\hat{Q}_t^a T_{tu}^{ab} \hat{Q}_u^b$ , where  $a$  and  $b$  denote (atomic) sites and  $t$  and  $u$  are multipole indices—00 for the charge, 10, 11c, and 11s for the components of the dipole, and so on.  $\hat{Q}_t^a$  is the multipole moment operator for moment  $t$  of site  $a$  and  $T_{tu}^{ab}$  are the interaction tensors that contain the distance and angular dependence (see Ref. 1 for details). Inserting this expansion in Eq. (7) we obtain the multipole form for the dispersion energy

$$E_{\text{disp}}^{(2)} = -\frac{1}{2\pi} T_{tu}^{ab} T_{t'u'}^{a'b'} \int_0^\infty \alpha_{tt'}^{aa'}(i\omega) \alpha_{u'u'}^{bb'}(i\omega) d\omega. \quad (8)$$

Here  $T_{tu}^{ab}$  is the interaction function between multipole  $t$  on site  $a$  in subsystem  $A$  and multipole  $u$  on site  $b$  in  $B$  while  $\alpha_{tt'}^{aa'}$  are the frequency-dependent nonlocal polarizabilities for sites  $a$  and  $a'$  and may be expressed in terms of the frequency-dependent density susceptibility as<sup>22</sup>

$$\alpha_{tt'}^{aa'}(\omega) = \int_a \int_{a'} \hat{Q}_t^a(\mathbf{r}) \alpha(\mathbf{r}, \mathbf{r}' | \omega) \hat{Q}_{t'}^{a'}(\mathbf{r}') d^3\mathbf{r} d^3\mathbf{r}'. \quad (9)$$

There are no assumptions made in deriving Eq. (8), other than that spheres enclosing the atomic charge densities on different molecules do not overlap. We have calculated distributed polarizabilities using the constrained density-fitting algorithm.<sup>22</sup>

Equation (8) involves a quadruple sum over sites and is therefore computationally demanding. To reduce this cost, we normally make a simplification by *localizing* the nonlocal polarizabilities. That is, the nonlocal polarizabilities—the  $\alpha_{tt'}^{aa'}(\omega)$  with  $a \neq a'$ —are transformed onto one or other site using the multipole expansion.<sup>23,24</sup> This transformation is possible only if the nonlocal terms decay fast enough with intersite distance. If not, the multipole expansion used in the transformation diverges and the localization is no longer possible. As we shall see, this is precisely what happens in the  $(\text{H}_2)_n$  chains as the distortion parameter  $\eta$  decreases.

An important feature of the nonlocal polarizability description is the presence of *charge-flow* polarizabilities—terms with  $t$  or  $u=00$  that describe the flow of charge in a molecule—which are usually small and die off quickly with distance. The lowest rank charge-flow polarizability is  $\alpha_{00,00}^{aa'}$ : if  $V^a$  is the potential at site  $a$ , the change in charge at site  $a$  is given by  $\Delta \hat{Q}_{00}^a = -\sum_{a'} \alpha_{00,00}^{aa'} (V^{a'} - V^a)$ . For a system with a large HOMO-LUMO gap the charge-flow terms are expected to be short range. The charge-flow polarizabilities of the  $(\text{H}_2)_{32}$  chain with  $\eta=2.0$  can be empirically modeled reasonably well with an exponential, that is,

$$\alpha_{00,00}^{aa'} \sim e^{-\gamma|r_{aa'}|}, \quad (10)$$

where  $r_{aa'}$  is the intersite distance and  $\gamma \approx 0.5$  a.u. In this case, the charge-flow polarizabilities drop by more than an order of magnitude within a few bonds. This is illustrated in Fig. 4. However, as we reduce the distortion parameter  $\eta$  the

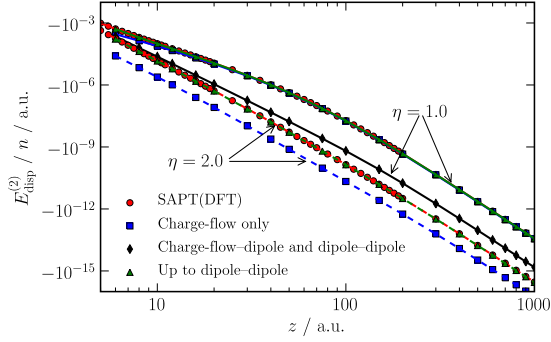


FIG. 5. (Color online) The second-order dispersion energy calculated using the polarizabilities of  $(\text{H}_2)_{32}$  chains with distortion parameters  $\eta=1$  and 2. The contribution from the charge-flow polarizabilities,  $\alpha_{00,00}^{aa'}$ , is displayed separately from the sum of contributions up to the dipole-dipole polarizabilities.

charge-flow polarizabilities decay more and more slowly with site-site distance, until, at  $\eta=1.0$ , they span the entire length of the chain. Even for the  $\eta=1.5$  chain, these nonlocal charge-flow polarizabilities can no longer be localized without incurring a significant error, but for the chains with  $\eta=1.25$  and 1.0 localization results in a qualitatively incorrect physical picture.

Moreover the charge-flow polarizabilities contribute to the dipole-dipole polarizability in the direction of the chain, and this contribution increases dramatically as the band gap decreases. For a 64-atom  $\text{H}_2$  chain with  $\eta=2$ , the static dipole polarizability  $\alpha_{xx}=\alpha_{11c,11c}$  parallel to the chain, calculated as described above, is about 410 a.u., of which 180 a.u. is contributed by charge flows. When  $\eta=1$ , so that the H atoms are equally spaced,  $\alpha_{xx}$  is about 11350 a.u., larger by about two orders of magnitude, and all of this increase is attributable to the charge-flow effects.

We have calculated the dispersion energy using Eq. (8) with distributed polarizabilities, including terms to rank 1. Higher ranking terms can be included, but these are not needed for the hydrogen chains. These results are presented in Fig. 5 for the  $(\text{H}_2)_{32}$  chains with  $\eta=2.0$  and 1.0. First of all, consider the insulating chain ( $\eta=2.0$ ): the charge-flow polarizabilities alone severely underestimate the dispersion energy, but when terms up to rank 1 are included the agreement of Eq. (8) with the nonexpanded SAPT(DFT) value for  $E_{\text{disp}}^{(2)}$  is excellent for all interchain separations shown in the figure. However, at  $\eta=1$ , the dispersion interaction is entirely dominated by the pure charge-flow (i.e.,  $\alpha_{00,00}^{aa'}$ ) terms, the higher order terms involving the dipole polarizabilities making a negligible contribution. Since the overall dispersion interaction is greatly enhanced as  $\eta$  is reduced, this implies that these pure charge-flow terms enhance the dispersion interaction in this limit.

Why do the charge-flow terms result in the anomalous power laws? The lowest rank charge-flow terms,  $\alpha_{00,00}^{aa'}$ , that appear in Eq. (8) are associated with  $T$  functions for the charge-charge interaction:  $T_{00,00}^{ab}=R_{ab}^{-1}$ , where  $R_{ab}$  is the distance between site  $a$  on one wire and site  $b$  on the other. If the wires are separated by distance vector  $\mathbf{R}=(0,0,z)$  and  $\mathbf{x}_a$  and  $\mathbf{x}_b$  are distance vectors for sites  $a$  and  $b$  along the chains

then  $\mathbf{R}_{ab}=\mathbf{R}-(\mathbf{x}_a-\mathbf{x}_b)$ . The dispersion energy arising from just the charge-flow terms is

$$E_{\text{disp}}^{(2)}(00,00) = -\frac{1}{2\pi} \sum_{aa'} \sum_{bb'} \frac{1}{R_{ab}} \frac{1}{R_{a'b'}} \times \int_0^\infty \alpha_{00,00}^{aa'}(iw) \alpha_{00,00}^{bb'}(iw) dw. \quad (11)$$

In contrast to the dipole-dipole polarizabilities, the charge-flow polarizabilities satisfy the sum rule  $\sum_{a'} \alpha_{t,00}^{aa'}(w)=0$ , which is a direct consequence of the charge-conservation requirement:  $\int \alpha_A(\mathbf{r}, \mathbf{r}'; w) d^3 \mathbf{r}' = 0$ . This leads to cancellation between the charge-flow contributions to the total dispersion energy and to a  $R^{-6}$  distance dependence at long range, but the cancellation is incomplete at short range, and terms in  $R^{-n}$ ,  $2 \leq n \leq 5$  also occur. To see how this arises, consider the following length scales: (1)  $L_c=1/\gamma$ , which is a measure of the extent of the charge fluctuations determined by the exponential decay of the charge-flow polarizabilities assumed in Eqs. (2) and (10)  $L$ , the chain length.

$z \leq L_c$ : Here the charge-flow terms dominate and contribute  $R^{-2}$  terms to the dispersion energy. From Fig. 4 we see that  $L_c$  is largest for the near-metallic wire for which we see the effects of these terms (Fig. 5) to  $z \sim 60$  a.u.

$L_c \ll z < L$ : In this region the extent of the charge fluctuations is small compared with  $R_{ab}$  and only those  $R_{a'b'}$  close to  $R_{ab}$  are important. We can therefore expand  $R_{a'b'}$  about  $R_{ab}$  using the multipole expansion. The leading term in this expansion is

$$E_{\text{disp}}^{(2)}(00,00) \approx -\frac{1}{2\pi} \sum_{ab} \frac{1}{R_{ab}} \frac{1}{R_{ab}} \int_0^\infty \left( \sum_{a'} \alpha_{00,00}^{aa'}(iw) \right) \times \left( \sum_{b'} \alpha_{00,00}^{bb'}(iw) \right) dw = 0, \quad (12)$$

where we have used the charge-flow sum rule. So we see that the  $R^{-2}$  contributions sum to zero in this region. However, the higher order contributions are nonzero.

$L \ll z$ : In this limit both  $R_{ab}$  and  $R_{a'b'}$  can be expanded in a multipole expansion about  $\mathbf{R}=(0,0,z)$ :  $R_{ab}^{-1}=|\mathbf{R}-(\mathbf{x}_a-\mathbf{x}_b)|^{-1}=|\mathbf{R}-\mathbf{x}_{ab}|^{-1} \approx z^{-1} - \frac{1}{2} x_{ab}^2 z^{-3}$ , and likewise for  $R_{a'b'}^{-1}$ . Once again, the leading terms vanish because of the sum rule, leaving only the effective dipole-dipole contribution

$$E_{\text{disp}}^{(2)}(00,00) \approx -\frac{1}{2\pi} \frac{1}{4z^6} \sum_{aa'} \sum_{bb'} x_{ab}^2 x_{a'b'}^2 \times \int_0^\infty \alpha_{00,00}^{aa'}(iw) \alpha_{00,00}^{bb'}(iw) dw \equiv -\frac{C_6(00,00)}{z^6}. \quad (13)$$

This explains the large- $z$  charge-flow contribution to the dispersion energy shown in Fig. 5. Notice that for the near-metallic wires, this contribution to the total molecular  $C_6$  coefficient dominates that from the dipole-dipole polarizabil-

ities but for the large-gap wires the opposite is true.

In short, the charge-flow polarizabilities give rise to the changes in power law of the dispersion energy and also contribute to an enhancement of the effective  $C_6$  coefficient, applicable at long range.

## V. DISCUSSION

The physical picture which emerges from both the Hückel approach and the *ab initio* calculations is the following. (1) In systems with a finite but small gap, spontaneous charge fluctuations (plasmon modes in the infinite case) introduce a secondary length scale intermediate in size to the interatomic distance and the system size. This length scale grows as the gap gets smaller. (2) For separations  $z$  small compared with this length scale, the dispersion energy arising from the correlated fluctuations has metallic character. (3) At  $z$  that are large compared with the length scale of the fluctuations, the dispersion can be described using London's dipole approximation, giving  $z^{-5}$  behavior, but the magnitude of the fluctuations now depends strongly on the band gap, leading to orders of magnitude enhancement over the insulator case.

(4) In small-gap systems these fluctuations give rise to a strong nonadditivity in the polarizability. For example, the ratio of the longitudinal static polarizabilities for the near-metallic and insulating  $(\text{H}_2)_{32}$  chains is 28. The dispersion energy is proportional to the square of the polarizability, that is, 784. This is roughly the ratio of the dispersion energies for these two cases but only at separations  $z$  much greater than the chain length. Any attempt to extrapolate this result to shorter distances results in a severe overestimation of the dispersion energy.

(5) This effect is not a consequence of retardation (we use the nonrelativistic Hamiltonian) or damping (charge-density overlap is negligible). It originates from the complex behavior of the nonlocal charge-flow polarizabilities. These are terms of rank zero that describe charge fluctuations in the system and are associated with a delocalized exchange-correlation hole.<sup>25,26</sup> This delocalization can be quantified using the localization tensor<sup>26,27</sup> and may give us a quantitative method for defining the charge-fluctuation length scale,  $L_c$ . We are currently investigating this possibility. (6) We have demonstrated that both the change in power law with distance and the enhancement of the dispersion energy can be understood using nonlocal polarizability models containing charge-flow polarizabilities. (7) It should come as no surprise that these effects are also strongly dependent on system size (see Fig. 3).

These results call into question theoretical methods that impose locality so as to scale linearly with system size (such as local coupled cluster and local MP2 methods) or that approximate the dispersion energy using a pair-wise  $-C_6R^{-6}$  interaction, as is done with dispersion-corrected DFT methods and empirical potentials. In the former, these effects can

be included by extending the region of locality, though at the cost of losing linearity in scaling, but the latter methods should not be applied to systems such as these. Even DFT functionals with a nonlocal dispersion correction, such as the van der Waals functional of Dion *et al.*<sup>28</sup> and the more recent functional of Vydrov and Van Voorhis<sup>29</sup> are unlikely to contain the correct physics because of an implicit assumption of locality in the polarizability. These functionals will include many-body nonadditive effects between nonoverlapping systems but not the nonadditive effects *within* each system such as those described here. On the other hand, methods based on the random-phase approximation and quantum Monte Carlo should be able to describe the nonadditive effects described in this paper if finite-size effects are kept under control.

In systems containing carbon atoms, such as  $\pi$ -conjugated chains, the contributions from the core electrons will at least partially mask those from the more mobile  $\pi$  electrons, so it is possible that the changes in power law of the dispersion interaction will not be as dramatic as those we see in the  $(\text{H}_2)_n$  chains. But we should nevertheless expect a high degree of nonadditivity arising from the charge-flow terms. One indicator of this nonadditivity is the nonlinear dependence of the molecular polarizability on system size. This has been already demonstrated above and is further supported by the experimental work of Compagnon *et al.*<sup>30</sup> on the polarizabilities of the fullerenes  $\text{C}_{70}$  and  $\text{C}_{60}$  which are found to be in the ratio 1.33 rather than the ratio  $70/60 = 1.17$  that would be expected if the systems were additive. Therefore, if reliable  $C_6$  models are to be constructed for extended  $\pi$ -conjugated systems, these models will need to absorb the effects of the nonadditivity of the charge-flow polarizabilities. That is, they should be tailored to suit the electronic structure of the system rather than be *transferred* from calculations on smaller systems. The Williams-Stone-Misquitta (WSM) procedure<sup>31-33</sup> is one such method that is capable of constructing effective local polarizability and dispersion models that account for the electronic structure of the system. In fact, the nonlocal models presented in this paper are derived in the first step of the WSM procedure. We are currently investigating the behavior of WSM dispersion models for a variety of carbon systems.

Finally, strongly delocalized systems will also have important contributions to the dispersion energy from terms of third order in the interaction operator, that is, from the hyperpolarizabilities. We have not considered such terms in this paper. Furthermore, in ensembles of such systems there will be strong nonadditive effects *between* molecules. We are currently investigating the nature and importance of this type of nonadditivity.

## ACKNOWLEDGMENTS

We thank University College London for computational resources. A.J.M. and J.S. thank EPSRC for funding.

- <sup>1</sup>A. J. Stone, *The Theory of Intermolecular Forces* (Clarendon Press, Oxford, 1996).
- <sup>2</sup>H. B. G. Casimir and D. Polder, *Phys. Rev.* **73**, 360 (1948).
- <sup>3</sup>J. F. Dobson, *Surf. Sci.* **601**, 5667 (2007).
- <sup>4</sup>J. F. Dobson, A. White, and A. Rubio, *Phys. Rev. Lett.* **96**, 073201 (2006).
- <sup>5</sup>J. F. Dobson, K. McLennan, A. Rubio, J. Wang, T. Gould, H. M. Le, and B. P. Dinte, *Aust. J. Chem.* **54**, 513 (2001).
- <sup>6</sup>J. F. Dobson, J. Wang, B. P. Dinte, K. McLennan, and H. M. Le, *Int. J. Quantum Chem.* **101**, 579 (2005).
- <sup>7</sup>N. D. Drummond and R. J. Needs, *Phys. Rev. Lett.* **99**, 166401 (2007).
- <sup>8</sup>J. Spencer, Ph.D. thesis, University of Cambridge, 2009.
- <sup>9</sup>P. Epstein, *Mathematische Annalen* **56**, 615 (1903).
- <sup>10</sup>P. Epstein, *Mathematische Annalen* **63**, 205 (1906).
- <sup>11</sup>M. P. Tosi, *Cohesion of Ionic Solids in the Born Model*, Solid State Physics Vol. XVI (Academic Press, New York, 1964).
- <sup>12</sup>A. J. Misquitta, B. Jeziorski, and K. Szalewicz, *Phys. Rev. Lett.* **91**, 033201 (2003).
- <sup>13</sup>A. Heßelmann, G. Jansen, and M. Schütz, *J. Chem. Phys.* **122**, 014103 (2005).
- <sup>14</sup>A. J. Misquitta, R. Podeszwa, B. Jeziorski, and K. Szalewicz, *J. Chem. Phys.* **123**, 214103 (2005).
- <sup>15</sup>H. C. Longuet-Higgins, *Discuss. Faraday Soc.* **40**, 7 (1965).
- <sup>16</sup>C. Adamo and V. Barone, *J. Chem. Phys.* **110**, 6158 (1999).
- <sup>17</sup>A. Heßelmann and G. Jansen, *Phys. Chem. Chem. Phys.* **5**, 5010 (2003).
- <sup>18</sup>R. Podeszwa and K. Szalewicz, *Chem. Phys. Lett.* **412**, 488 (2005).
- <sup>19</sup>B. Champagne, E. A. Perpete, S. J. A. van Gisbergen, E.-J. Baerends, J. G. Snijders, C. Soubra-Ghaoui, K. A. Robins, and B. Kirtman, *J. Chem. Phys.* **109**, 10489 (1998).
- <sup>20</sup>H. Sekino, Y. Maeda, M. Kamiya, and K. Hirao, *J. Chem. Phys.* **126**, 014107 (2007).
- <sup>21</sup>T. H. Dunning, Jr., *J. Chem. Phys.* **90**, 1007 (1989).
- <sup>22</sup>A. J. Misquitta and A. J. Stone, *J. Chem. Phys.* **124**, 024111 (2006).
- <sup>23</sup>C. R. Le Sueur and A. J. Stone, *Mol. Phys.* **83**, 293 (1994).
- <sup>24</sup>T. C. Lillestolen and R. J. Wheatley, *J. Phys. Chem. A* **111**, 11141 (2007).
- <sup>25</sup>J. G. Ángyán, *J. Chem. Phys.* **127**, 024108 (2007).
- <sup>26</sup>J. G. Ángyán, *Int. J. Quantum Chem.* **109**, 2340 (2009).
- <sup>27</sup>R. Resta and S. Sorella, *Phys. Rev. Lett.* **82**, 370 (1999).
- <sup>28</sup>M. Dion, H. Rydberg, E. Schroder, D. C. Langreth, and B. I. Lundqvist, *Phys. Rev. Lett.* **92**, 246401 (2004).
- <sup>29</sup>O. A. Vydrov and T. VanVoorhis, *Phys. Rev. Lett.* **103**, 063004 (2009).
- <sup>30</sup>I. Compagnon, R. Antoine, M. Broyer, P. Dugourd, J. Lerme, and D. Rayane, *Phys. Rev. A* **64**, 025201 (2001).
- <sup>31</sup>A. J. Misquitta and A. J. Stone, *J. Chem. Theory Comput.* **4**, 7 (2008).
- <sup>32</sup>A. J. Misquitta, A. J. Stone, and S. L. Price, *J. Chem. Theory Comput.* **4**, 19 (2008).
- <sup>33</sup>A. J. Misquitta and A. J. Stone, *Mol. Phys.* **106**, 1631 (2008).